Structures and Mechanical Properties of ECAP Processed 7075 Al Alloy upon Natural Aging and T651 Treatment

Yonghao Zhao[1], Xiaozhou Liao[1], Ruslan Z. Valiev[2] and Yuntian T. Zhu[1]
[1]Materials Science and Technology Division, Los Alamos National Laboratory, Los Alamos, NM-87545, U.S.A.
[2]Institute of Physics of Advanced Materials, Ufa State Aviation Technical University, 12 K. Marx Street, 450000 Ufa, Russian Federation

ABSTRACT

Equal-channel angular pressing (ECAP) processed ultrafine grained (UFG) and coarse grained (CG) 7075 Al alloys were treated by natural aging and T651 temper (annealed at 120 ºC for 48 h in Ar atmosphere), respectively. Mechanical tests showed that for the UFG sample, the natural aging resulted in the highest strength (the ultimate tensile strength is 720 MPa). In contrast, for the CG sample, the T651 treatment resulted in a higher strength (the ultimate strength is 590 MPa) than the natural aging (530 MPa). Microstructural analyses indicated that the enhanced strength of the T651 treated CG sample was mainly caused by high densities of G-P zones and metastable η′ precipitates. The enhanced strength of the naturally aged UFG sample was mainly caused by the high densities of G-P zones and dislocations. Upon T651 treatment, the dislocation density of the UFG sample deceased significantly, overcompensating the precipitation strengthening.

INTRODUCTION

In the last decade, equal channel angular pressing (ECAP) technique has been widely used to produce bulk ultrafine grained (UFG) metal and alloys, such as Al and its alloys, Cu, Ni, Ti and its alloys, and steels. During an ECAP process, the sample is deformed by being pressed through a die containing two channels, equal in cross section and intersecting at a certain angle. The bulk UFG materials are thought to have considerable potential for industrial applications due to their high strength with good ductility, superplasticity at moderate temperatures and high strain rates, etc. [1].

For Al alloys, most ECAP effort has focused on work strengthening Al-Mg alloys [2-5]. Much less attention has been paid to the precipitate hardening Al-Zn-Mg 7000 series alloys [6,7], which show the highest strength of all commercial Al alloys and are widely used for structural applications in military and civil aircraft as well as sporting goods. Conventional cold working, which usually improves the strength of metals and alloys, has been found to be ineffective in improving the strength of 7000 series Al alloys [8]. It is of great interest to investigate if the strengthening effect observed in ECAP-processed UFG materials can be added to the precipitation hardening effect in the 7000 series Al alloys. If these two strengthening effects can be made additive, it will be possible to significantly improve the strength of 7000 Al alloys, making them much more attractive in high strength structural applications.

In the literature, the highest strength of the 7000 Al alloys was obtained by a T651 temper (annealing at 120 °C for 24 h after solution treatment). T651 treatment produced high densities of coherent spherical-shaped G-P zones and semicoherent intermediate metastable η′ phase, which increase the resistance to dislocation movement arising from the strong atomic bonds in

the zones [8]. The objective of this work was to investigate the microstructures and mechanical properties of naturally aged (NA) and T651 treated UFG 7075 Al alloy produced by ECAP process. For comparison, coarse-grained (CG) 7075 samples, subjected to the same natural aging and T651 temper, were also characterized.

EXPERIMENTAL DETAILS

Commercial 7075 Al alloy was homogenized by solution treatment for 5 h at 480 °C and quenched to room temperature. The initial grain size is approximately 40 μm. An ECAP die with an intersecting channel angle of 90º and an outerarc angle of 45° was used. The sample was processed for 2 passes by route B_c in which the work piece was rotated 90° along its longitudinal axis between adjacent passes. The ECAP processed UFG and initial solution-treated CG 7075 Al alloys were naturally aged at room temperature for one month and aged at 120 ºC for 24 h (T651 temper), then were cut into small pieces in an orientation perpendicular to the pressing direction. The surfaces of these thin pieces were polished for subsequent characterization.

Tensile tests were carried out using a Shimadzu Universal Tester. The samples were cut and polished into a 2.0 mm×1.4 mm cross section and a gauge length of 18.0 mm for tensile tests (in an orientation parallel to the pressing direction) at a displacement rate of 1×10^{-2} mm/s. Microhardness measurements were carried out on Buehler Micromet® Hardness Tester with a load of 500 g and loading time of 15 s. The indenter is the Vickers diamond pyramid. For each sample, at least 20 points were measured to obtain an average value with a typical uncertainty of ±2 %.

Quantitative x-ray diffraction (XRD) measurements were performed on a Scintag x-ray diffractometer, which was equipped with a Cu target operating at 1.8 kW and a secondary monochromator to select the Cu K_α radiation. θ-2θ scans with a step size of $2\theta = 0.02°$ and a counting time of 10 s were performed at room temperature. Pure Al powder (99.999%) was annealed at 200 ºC in Ar and used as a XRD reference. Transmission electron microscopy (TEM) and high-resolution transmission electron microscopy (HREM) were performed using a Phillips CM30 microscope operating at 300 kV and a JEOL 3000F microscope operating at 300 kV, respectively. The TEM and HREM samples were prepared by mechanical grinding of the 7075 Al alloy disks to a thickness of about 10 μm. Further thinning to a thickness of electron transparency was carried out using a Gatan Dual Ion Milling System with an Ar+ accelerating voltage of 4 kV and liquid nitrogen for cooling the specimens.

EXPERIMENTAL RESULTS

The engineering stress-strain curves of the UFG and CG samples are shown in figure 1. Upon natural aging, the tensile yield strength, σ_{ys}, and ultimate strength, σ_{us}, of the UFG sample are 650 MPa and 720 MPa, respectively, which are about 103% and 35% higher, respectively, than those of the CG sample (320 MPa and 530 MPa). The elongation to failure of the UFG sample (8.4%) is smaller than that of the CG sample (20.5%). Upon T651 temper, the σ_{ys} and σ_{us} of the UFG sample decreased to 550 MPa and 600 MPa, respectively, while the σ_{ys} and σ_{us} of the CG sample increased to490 MPa and 590 MPa, respectively. The present mechanical properties of the CG sample agree well with the literature [9]. The Vickers microhardness of the natural aged UFG sample (201 H_V) is about 48% larger than that of CG sample (136 H_V). Upon T651

treatment, the hardness of the UFG sample decreased to 178 H_V, while that of the CG sample increased to 174 H_V.

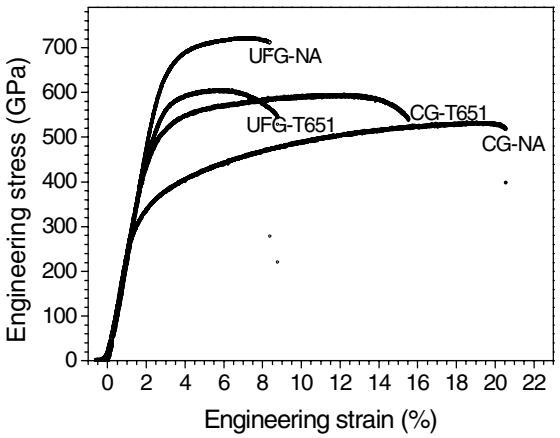

Figure 1. The engineering stress-strain curves of the UFG and CG samples treated by natural aging (NA) and T651 temper.

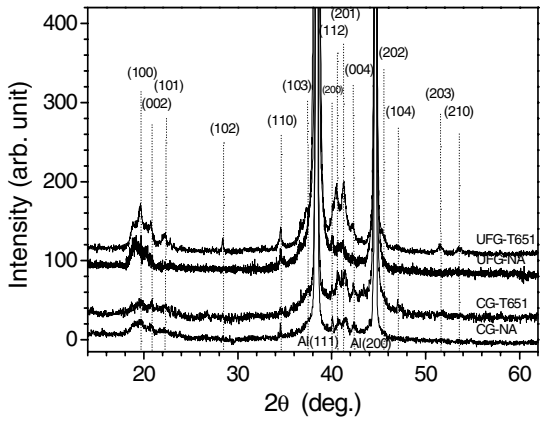

Figure 2. XRD patterns of the UFG and CG samples treated by natural aging (NA) and T651 temper.

Table I. The tensile yield stresses (σ_{ys}), ultimate stresses (σ_{us}), ultimate elongation (ε_{ue} and Vickers microhardnesses (DPH, H_V) of the naturally aged and T651 treated UFG and CG 7075 Al alloys.

	UFG-NA	UFG-T651	CG-NA	CG-T651
σ_{ys} (MPa)	650	550	320	490
σ_{us} (MPa)	720	600	530	590
ε_{ue} (%)	8.4	8.8	20.5	15.5
H_V/0.5, DPH	201	178	136	174

The XRD patterns of the UFG and CG samples treated by natural aging and T651 temper are shown in figure 2. The indexes of diffraction planes of the metastable hexagonal η′ were also indicated in the figure. The UFG and CG samples have similar variations in the x-ray patterns upon natural aging and T651 temper. For the naturally aged UFG and CG samples, besides Al reflections, there appeared a broad peak at about $2\theta = 20°$ and some other weak peaks. The broad peak at about 20° corresponds to the G-P zones [10], and the other weak peaks are from the metastable η′ phase. Upon T651 temper, there precipitated large amount of η′ phase coexisted with G-P zones. Because the XRD sample has the same area involved in the reflection, the intensity of the XRD patterns can be compared. From figure 2, the intensity of the G-P zone broad peak of the naturally aged UFG sample is larger than that of the naturally aged CG sample, indicating that the volume fraction of the G-P zones in the naturally aged UFG sample is larger than that in the naturally aged CG sample. Similarly, the volume fractions of the G-P zones and metastable η′ phase in the T651 treated UFG sample are larger than those in the T651 treated CG sample.

The above-mentioned phase precipitations in the UFG and CG samples can also be observed by TEM and HREM, as shown in figures 3 (a-d). The HREM pictures were observed from a

[110] direction of the Al matrix. For the naturally aged UFG and CG samples, both spherical G-P zones (as indicated by arrows in the inset in figure 3a) and plate-shaped η′ (see the inset in figure 3c) are observed. The volume fraction of the G-P zones in the naturally aged UFG sample is larger than that in the CG sample by numerous observations in different areas, which agrees with the XRD results. After T651 temper (figures 3b and 3d), a large amount of plate-shaped η′ phase precipitated out and mixed with the G-P zones. The volume fractions of the G-P zones and metastable hexagonal η′ phase in the UFG sample are larger than those in the CG sample, agreeing with XRD results.

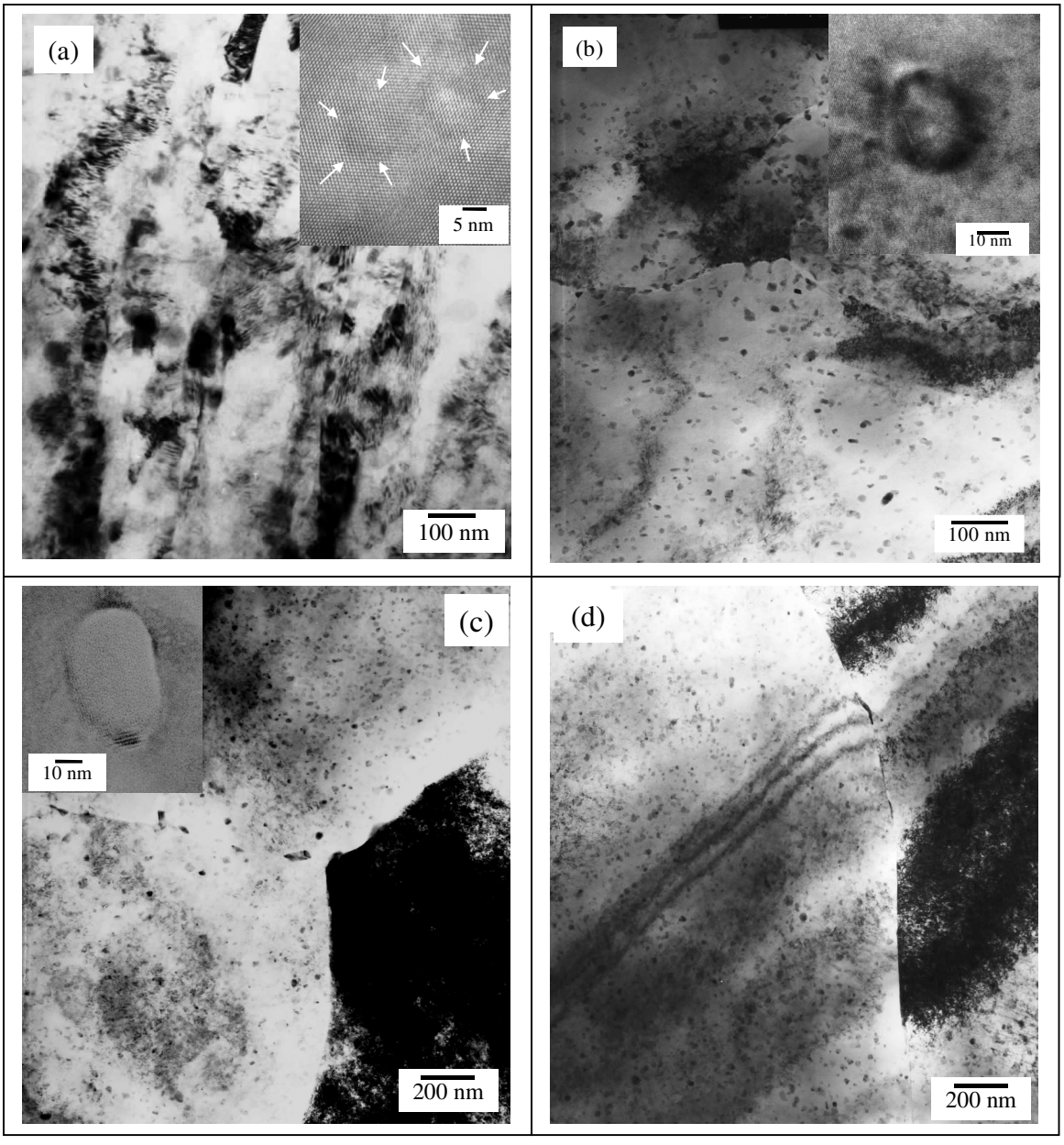

Figure 3. TEM and HREM pictures of the UFG (a,b) and CG (c,d) samples treated by natural aging (a,c) and T651 temper (b,d).

From TEM pictures, one can obtain the average grain size (see Table II). TEM showed that the naturally aged UFG sample was composed of lamella grains with a length of about 430 nm and a width of about 150 nm, which was produced by shear deformation during the ECAP process (figure 3a). Upon T651 temper, the lamella-grains grew into equiaxed grains with a size of about 2 μm. The grain sizes of the naturally aged and T651 treated CG samples were about 40 and 50 μm, respectively. The grain size and microstrain can also be calculated from XRD broadening peaks by the Scherrer and Wilson method [11], as listed in Table II. The XRD calculated grain size is smaller than that from TEM, because XRD gives the scattering domain size or sub-grain size. From the XRD results, the grain size of the naturally aged UFG sample is about 70 nm. The microstrain of the naturally aged UFG sample was 0.54 %, and it decreased significantly to 0.25 % upon T651 temper. The microstrains of the naturally aged and T651 treated CG samples were about 0.05 %.

Table II. The average grain sizes calculated from TEM pictures (D), microstrains ($\langle\varepsilon^2\rangle^{1/2}$) and dislocation densities (ρ) of the naturally aged and T651 treated UFG 7075 Al alloy and the CG 7075 Al counterpart.

Samples	UFG-NA	UFG-T651	CG-NA	CG-T651
D (nm)	290	1,900	42,000	49,000
$\langle\varepsilon^2\rangle^{1/2}$ (%)	0.54	0.25	0.05	0.08
ρ (10^{15} m^{-2})	0.94	0.02	0.0	0.0

The dislocation densities in the UFG and CG samples can be calculated from the grain size and microstrain [12,13], as listed in Table II. The dislocation density of the naturally aged UFG sample was about 0.94×10^{15} m^{-2}, and it decreased significantly to about 0.02×10^{15} m^{-2} upon T651 temper. For the naturally aged and T651 treated CG samples, the dislocation densities remained at about zero.

DISCUSSION

The strength of the naturally aged UFG 7075 alloy is significantly higher than its naturally-aged CG counterparts, indicating that it is possible to add strengthening from ECAP processing to that from precipitation hardening.

The significantly high strength of the UFG 7075 Al alloy may be attributed to (i) solid solution strengthening, (ii) grain refinement strengthening, (iii) dislocation strengthening and (iv) precipitation strengthening. The first two effects appear to have less contribution compared to the last two effects, which were verified elsewhere [14]. The XRD analysis revealed high dislocation density in the naturally aged UFG sample, suggesting that dislocation strengthening has a significant contribution to the strength enhancement. The dislocation networks and tangles within grains and near grain or sub-grain boundaries make dislocation glide more difficult. The precipitation strengthening results from the precipitate's ability to impede dislocation motion by forcing dislocations to either cut through or circumvent the fine precipitates. In either case, higher density of precipitates leads to higher strength. For naturally aged 7075 Al alloy, the dislocation cutting of the G-P zones and η′ fine plates is the main strengthening mechanism, because the strong atomic bonds in the zones can effectively hinder dislocation motion [8]. Both XRD and HREM revealed that the volume fraction of the G-P zones in the UFG sample is larger

than that in the CG sample. Therefore, the cooperative interaction of the high densities of the G-P zones and dislocations has resulted in the observed significantly higher strength of the naturally aged UFG 7075 Al alloy. The enhanced strength of the T651 treated CG sample was mainly caused by high densities of G-P zones and metastable η′ precipitates. Upon T651 treatment, the dislocation density of the UFG sample deceased significantly, overcompensating the precipitation strengthening.

CONCLUSION

A combination of ECAP processing and precipitation hardening has the potential to render Al 7000 series alloys significantly stronger than those processed by either technique alone. The high densities of G-P zones and dislocations are primarily responsible for the high strength of naturally-aged UFG 7075 alloy. A T651 temper resulted in the high strength of the CG sample, caused by high densities of G-P zones and metastable η′ precipitates. However, a T651 temper decreased the strength of the UFG sample, because the T651 treatment deceased the dislocation density significantly, overcompensating the precipitation strengthening.

REFERENCES

1. R.Z. Valiev, R.K. Islamgaliev and I.V. Alexandrov, Prog. Mater. Sci. **45**, 103 (2000).
2. J. Wang, Y. Iwahashi, Z. Horita, M. Furukawa, M. Nemoto, R.Z. Valiev and T.G. Langdon. Acta mater. **44**, 2973 (1996).
3. M. Furukawa, A. Utsunomiya, K. Matsubara, Z. Horita and T.G. Langdon, Acta mater. **49**, 3829 (2001).
4. S. Lee, A. Utsunomiya, H. Akamatsu, K. Neishi, M. Furukawa, Z. Horita and T.G. Langdon, Acta mater. **50**, 553 (2002).
5. D.G. Morris and M.A. Munoz-Morris, Acta mater. **50**, 4047 (2002).
6. Z. Horita, T. Fujinami, M. Nemoto and T.G. Langdon, Metall. Trans. **31A**, 691 (2000).
7. L.J. Zheng, C.Q. Chen, T.T. Zhou, P.Y. Liu and M.G. Zeng, Mater. Character. **49**, 455 (2003).
8. W.F. Smith, *Structure and Properties of Engineering Alloys*, (McGraw-Hill: New York, 1993) Chap. 5-9, p. 214.
9. Y. Murakami, Aluminum-Based Alloys, in *Processing Metals and Alloys*, edited by R.W. Cahn (VCH: Weinheim, New York, c1991), p. 253.
10. Y.H. Zhao, X.Z. Liao, Z. Jin, R.Z. Valiev and Y.T. Zhu, in *Ultrafine-Grained Materials III*, edited by Y.T. Zhu, T.G. Langdon, R.Z. Valiev, S.L. Semiatin, D.H. Shin and T.C. Lowe (The Minerals, Metals & Materials Society, 2004), p. 511.
11. Y.H. Zhao, K. Zhang and K. Lu, Phys. Rev. B, **56**, 14322 (1997).
12. Y.H. Zhao, H.W. Sheng and K. Lu, Acta mater. **49**, 365 (2001).
13. Y.H. Zhao, K. Zhang and K. Lu, Phys. Rev. B, **66**, 085404-01 (2002).
14. Y.H. Zhao, X.Z. Liao, Z. Jin, R.Z. Valiev and Y.T. Zhu, to be published in Acta mater. (2004).